S-nitrosylated TDP-43 triggers aggregation, cell-to-cell spread, and neurotoxicity in hiPSCs and in vivo models of ALS/FTD

Elaine Pirie[a,1], Chang-ki Oh[b,c,d,1], Xu Zhang[b,c,d], Xuemei Han[b,c,d], Piotr Cieplak[e], Henry R. Scott[b,c,d], Amanda K. Deal[b,c,d], Swagata Ghatak[b,c,d], Fernando J. Martinez[a], Gene W. Yeo[a], John R. Yates III[b,c,d], Tomohiro Nakamura[b,c,d,2], and Stuart A. Lipton[b,c,d,f,2]

[a]Department of Cellular and Molecular Medicine and Biomedical Sciences Graduate Program, University of California San Diego, La Jolla, CA 92093; [b]Department of Molecular Medicine, The Scripps Research Institute, La Jolla, CA 92037; [c]Department of Neuroscience, The Scripps Research Institute, La Jolla, CA 92037; [d]Neuroscience Translational Center, The Scripps Research Institute, La Jolla, CA 92037; [e]Bioinformatics and Structural Biology Program, Sanford Burnham Prebys Medical Discovery Institute, La Jolla, CA 92037; and [f]Department of Neurosciences, University of California San Diego School of Medicine, La Jolla, CA 92093

Edited by Louis J. Ignarro, The University of California, Los Angeles School of Medicine, Beverly HIlls, CA, and approved February 3, 2021 (received for review October 13, 2020)

Rare genetic mutations result in aggregation and spreading of cognate proteins in neurodegenerative disorders; however, in the absence of mutation (i.e., in the vast majority of "sporadic" cases), mechanisms for protein misfolding/aggregation remain largely unknown. Here, we show environmentally induced nitrosative stress triggers protein aggregation and cell-to-cell spread. In patient brains with amyotrophic lateral sclerosis (ALS)/frontotemporal dementia (FTD), aggregation of the RNA-binding protein TDP-43 constitutes a major component of aberrant cytoplasmic inclusions. We identify a pathological signaling cascade whereby reactive nitrogen species cause S-nitrosylation of TDP-43 (forming SNO-TDP-43) to facilitate disulfide linkage and consequent TDP-43 aggregation. Similar pathological SNO-TDP-43 levels occur in postmortem human FTD/ALS brains and in cell-based models, including human-induced pluripotent stem cell (hiPSC)-derived neurons. Aggregated TDP-43 triggers additional nitrosative stress, representing positive feed forward leading to further SNO-TDP-43 formation and disulfide-linked oligomerization/aggregation. Critically, we show that these redox reactions facilitate cell spreading in vivo and interfere with the TDP-43 RNA-binding activity, affecting SNMT1 and phospho-(p)CREB levels, thus contributing to neuronal damage in ALS/FTD disorders.

TDP-43 proteinopathy | S-nitrosylation | aggregation | spread

Identification of genetic, pathological, and clinical signatures of amyotrophic lateral sclerosis (ALS) and frontotemporal dementia (FTD) suggests a continuum of disease on a single ALS/FTD spectrum of disorders. At a genetic level, mutations in specific genes, including *TARDBP* (encoding the RNA-binding protein TDP-43), *fused-in-sarcoma* (*FUS*), and *valosin containing protein* (*VCP*), or hexanucleotide repeat expansion, as in *C9ORF72*, have been linked to ALS and/or FTD (1). Even in the absence of mutation, TDP-43 proteinopathy, involving cytoplasmic aggregation and consequent nuclear clearance of TDP-43 in affected cells, represents a major pathological hallmark appearing in 97% of ALS and 45% of FTD cases (2, 3). The high prevalence of TDP-43 proteinopathy in the face of rare genetic mutations in the *TARDBP* gene (representing only ∼4% of ALS cases) points to the possibility that other factors related to age or environment contribute to TDP-43 aggregation in the vast majority of patients with ALS/FTD spectrum disorders.

Under normal conditions, TDP-43 resides predominantly in the nucleus, functioning as an RNA-binding protein for regulation of mRNA processing and stabilization (4, 5). In contrast, in ALS/FTD, TDP-43 becomes highly phosphorylated, ubiquitinated, and insoluble and mislocalizes to the cytosol to form stress granules (SGs) (6). For example, enhanced activity of casein kinases and possibly other kinases, such as glycogen synthase kinase 3 and cyclin-dependent kinases, lead to hyperphosphorylation of TDP-43, promoting aggregation of TDP-43 in cytosolic SGs (7, 8). SGs are nonmembrane-bound organelles that can sequester specific mRNAs via phase separation (9) to inhibit the initiation of translation. Additionally, emerging evidence suggests that cell-to-cell spreading of pathological aggregates of TDP-43 contributes to the propagation of the proteinopathy (10–12). Prior reports support the notion that disease progression in TDP-43 proteinopathy can be mediated by aggregation-related loss-of-normal function (e.g., RNA binding in the nucleus) or gain-of-toxic function, or possibly both (13). Studies have also implicated microglia-dependent pathways in

Significance

Aggregation and cell-to-cell spread of TDP-43 are thought to underlie many cases of frontotemporal dementia (FTD) and amyotrophic lateral sclerosis (ALS). Additionally, the aging process and environmental toxins stimulate excessive generation of reactive oxygen and nitrogen species (ROS/RNS), thus contributing to the pathological processes of these neurodegenerative diseases. Here, we show that nitric oxide (NO)-related species promote TDP-43 proteinopathy in cell-based and animal models of FTD/ALS via S-nitrosylation of TDP-43 at critical cysteine residues that facilitate disulfide bond formation and abnormal aggregation of the protein. In contrast, expression of nonnitrosylatable mutant TDP-43 ameliorates TDP-43 aggregation, RNA binding, and cell toxicity. Thus, our study provides mechanistic insight into the ROS/RNS-induced TDP-43 proteinopathy and neurotoxicity observed in FTD/ALS patients.

Author contributions: E.P., C.-k.O., T.N., and S.A.L. designed research; E.P., C.-k.O., X.Z., X.H., P.C., H.R.S., A.K.D., S.G., F.J.M., and T.N. performed research; E.P., C.-k.O., X.Z., X.H., P.C., G.W.Y., J.R.Y., T.N., and S.A.L. analyzed data; and E.P., C.-k.O., X.H., P.C., T.N., and S.A.L. wrote the paper.

Competing interest statement: G.W.Y. is a cofounder of Locana and Eclipse Bioinnovations and a member of the scientific advisory boards of Locana, Eclipse Bioinnovations, and Aquinnah Pharmaceuticals. The terms of this arrangement have been reviewed and approved by the University of California San Diego in accordance with its conflict of interest policies. S.A.L. is a scientific cofounder of Adamas Pharmaceuticals, Inc. and EuMentis Therapeutics, Inc., as disclosed to the institutions with which he is academically affiliated and performs research in accordance with their conflict of interest policies.

This article is a PNAS Direct Submission.

[1]E.P. and C.-k.O. contributed equally to this work.

[2]To whom correspondence may be addressed. Email: tnakamura@scripps.edu or slipton@scripps.edu.

This article contains supporting information online at https://www.pnas.org/lookup/suppl/doi:10.1073/pnas.2021368118/-/DCSupplemental.

Published March 10, 2021.

TDP-43 proteinopathy (14). Furthermore, recent studies have revealed that TDP-43 pathology occurs in a wide variety of other neurodegenerative disorders, including Alzheimer's disease (AD), Parkinson's disease (PD), and Huntington's disease (HD) (15), suggesting a wider role for TDP-43 proteinopathy in neurodegeneration. However, mechanistic insight into the development and execution of TDP-43 pathology remains incompletely understood.

Two risk factors that have been strongly implicated in the pathogenesis of neurodegenerative disorders are the aging process and environmental toxins (16–19). Both of these risk factors engender dramatic increases in chemically reactive species, including reactive oxygen and nitrogen species (ROS/RNS) such as nitric oxide (NO), and it has been suggested that this may play a role in the degenerative process as observed in ALS/FTD (18–22). Along these lines, we and others have demonstrated that protein S-nitrosylation, resulting from posttranslational modification of cysteine thiol groups by NO-related species, contributes to protein misfolding, mitochondrial dysfunction, synaptic impairment, and eventually neuronal cell loss (19). Several chemical mechanisms for in vivo formation of protein S-nitrosylation have been proposed (23, 24). For example, cysteine thiol (or more properly thiolate anion) can perform a reversible nucleophilic attack on a nitroso nitrogen to form a protein S-nitrosothiol via transnitrosation or transnitrosylation (24, 25). Mechanism notwithstanding, protein S-nitrosylation is now well recognized as a major contributor to both the physiological and pathophysiological activity (19, 20).

Interestingly, the Food and Drug Administration (FDA)-approved drug edaravone (MCI-186) delays disease progression in some cases of ALS (26), possibly via scavenging RNS/ROS related to NO and hydroxyl radical groups (27, 28). While exogenous addition of ROS-generating agents has been reported to decrease the solubility of TDP-43 in vitro in cell-based models (29–31), endogenous reactive chemical species have not been previously reported to do this in a pathophysiologically relevant manner. Accordingly, in the present study, we report that not only exogenous but also endogenous RNS can trigger TDP-43 aggregation via S-nitrosylation and consequent disulfide bond formation; in models of FTD and ALS, we identify endogenous SNO-TDP-43 formation as a critical effector of pathological signaling, leading to its aggregation, altered RNA-binding activity, and neurotoxicity. Moreover, we find that increased expression of TDP-43 protein, as found in ALS, FTD, and other neurodegenerative disorders, results not only in misfolded/aggregated protein but also in dramatically increased NO production and additional protein misfolding/aggregation, representing a positive feed-forward loop to enhance nitrosative stress and thus protein misfolding. Additionally, we report that, in conjunction with NO, mutation in the *VCP* gene, as observed in some cases of ALS/FTD, triggers a dramatic increase in misfolded/aggregated TDP-43 in human-induced pluripotent stem cell (hiPSC)-derived motoneurons. Our results thus place TDP-43 at a unique node of intersection between genetic mutations associated with ALS/FTD and aging/environmental risk factors mediated by NO-related species, which together contribute to neurodegeneration in ALS/FTD spectrum disorders.

Results

S-Nitrosylation of TDP-43 in Cell-Based Models. While basal levels of NO act as a mediator of normal biological processes via enzymatic processes, pathologically increased production of NO exerts neurodestructive effects, at least in part through aberrant protein S-nitrosylation of critical cysteine thiol groups in an enzymatic or nonenzymatic fashion (19). Generally, NO-reactive cysteine residues reside in a motif that fosters S-nitrosylation (32), but as NO levels rise to pathological levels, often only a partial motif suffices (19). In a systematic search of pathologically misfolded proteins containing such motifs, we found candidate cysteines on TDP-43. Therefore, we initially tested if S-nitrosothiol formation occurs on TDP-43 (designated SNO-TDP-43) by exposing rat primary cerebrocortical cultures to the physiological NO donor, S-nitrosocysteine (SNOC). Note that both SNOC and S-nitrosoglutathione (GSNO) can serve not only as "NO donors" but can also transnitrosylate another thiol/thiolate for generation of an S-nitrosothiol. Thirty minutes after addition of SNOC, we performed the biotin-switch technique in which free thiols are blocked with methyl methanethiosulfonate (MMTS) and S-nitrosothiols are specifically reduced by ascorbate for subsequent labeling with biotin (33). Streptavidin pulldown followed by Western blot showed a significant increase in SNO-TDP-43 levels in cortical neurons incubated with SNOC (Fig. 1*A*).

Next, we examined if endogenously produced NO could lead to the generation of SNO-TDP-43. For this purpose, we utilized HEK-293 cells stably expressing neuronal NO synthase (HEK-nNOS); the biotin switch assay demonstrated that activation of nNOS by the calcium ionophore A23187 resulted in elevated levels of SNO-TDP-43 (Fig. 1*B*). To determine if S-nitrosylation of TDP-43 occurs under pathophysiologically relevant conditions, we stimulated *N*-methyl-D-aspartate-type glutamate receptors (NMDARs) on neurons in rat cerebrocortical cultures to induce endogenous NO generation. We employed this model since we and others had previously reported that NMDAR-mediated excitotoxicity contributes to neurodegeneration, at least in part, via NO-dependent signaling pathways (19, 22, 34, 35). Indeed, under these conditions we observed a significant increase in SNO-TDP-43 formation (Fig. 1*C*). These results are consistent with the notion that pathological levels of NO-related species can trigger S-nitrosylation of TDP-43.

S-Nitrosylation Contributes to TDP-43 Aggregation. Prior studies by our group and others have demonstrated that protein S-nitrosylation can alter protein conformation, thus contributing to protein aggregation (19, 35). To test if S-nitrosylation of TDP-43 increases oligomers and aggregation, we initially produced recombinant TDP-43 composed of amino acids 1 through 265 (TDP-43[1-265]). This recombinant protein encompasses all of the cysteine residues in TDP-43. Using the biotin-switch assay, we verified that recombinant TDP-43(1-265) undergoes S-nitroso-modification in vitro upon exposure to SNOC (Fig. 2*A*). When SNO-TDP-43(1-265) was subjected to top-down analysis by LTQ-orbitrap high-resolution mass spectrometry, we observed a 29-Da shifted peak, reflecting the addition of a NO group to a single cysteine residue (Fig. 2*B*; S-nitrosylation site shown in Fig. 3).

Having shown that TDP-43(1-265) can be S-nitrosylated, we then examined if this reaction results in dimerization/oligomerization of TDP-43. Following incubation with SNOC, we observed a significant increase in dimerized TDP-43(1-265) by sodium dodecyl sulfate polyacrylamide gel electrophoresis (SDS-PAGE) visualized with Coomassie blue staining (Fig. 2*C*). Notably, treatment with a reducing agent (e.g., β-mercaptoethanol) completely abrogated dimerization, suggesting that disulfide bond formation is involved in dimer formation. In fact, we and others have previously shown that S-nitrosylation of one of two neighboring cysteine residues can result in facile disulfide bond formation between the two vicinal thiol groups (19, 20, 36–38). To investigate if SNO-TDP-43 precipitates disulfide-mediated dimerization in intact neurons, we exposed rat cerebrocortical cultures to SNOC and collected cell lysates 10 and 40 min later. Immunoblot analyses with anti-TDP-43 antibody revealed formation of high molecular weight (HMW, including dimers) TDP-43 in a time-dependent manner (Fig. 2*D*); in contrast, SNO-TDP-43 formation peaked at 10 min after SNOC exposure and decreased thereafter. These results are consistent with the notion that SNO-TDP-43 represents the initial product of nitrosative stress and subsequently yields disulfide-mediated, HMW TDP-43 aggregates.

Previous examination of human patient brains with TDP-43 proteinopathy revealed that aggregated TDP-43 mislocalizes to cytoplasmic SGs, thus sequestering the protein and resulting in

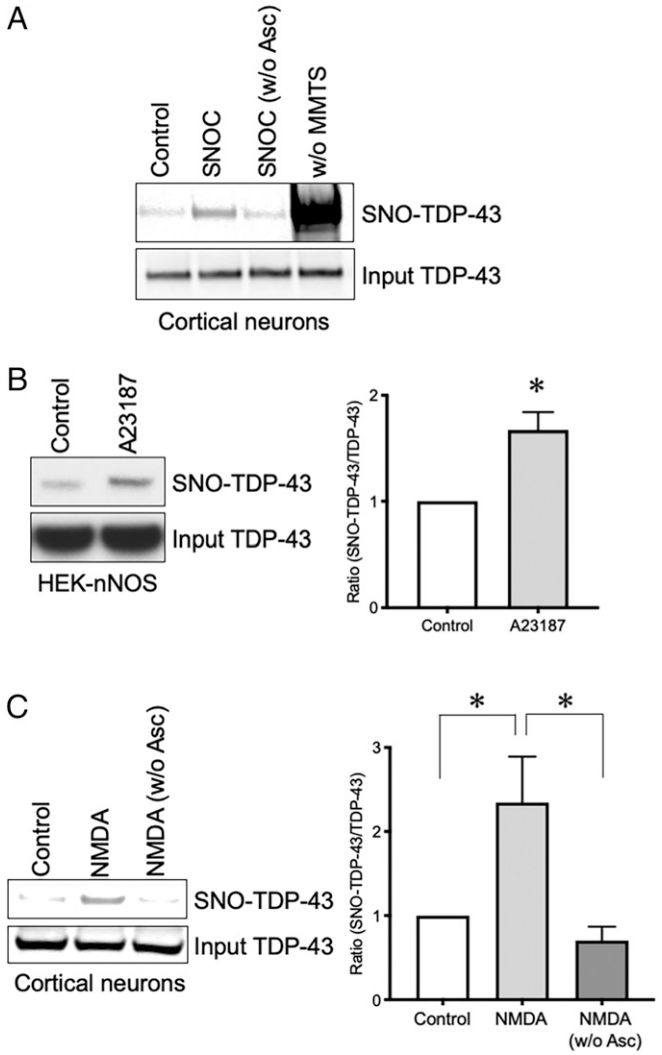

Fig. 1. TDP-43 is S-nitrosylated in cultured neuronal cells. (*A*) S-nitrosylation of TDP-43 in primary rat cerebrocortical neurons. Neurons were exposed to the NO donor SNOC (200 μM), and S-nitrosylation of TDP-43 (SNO-TDP-43) was assessed by biotin-switch assay. Samples without MMTS (w/o MMTS) or ascorbate (w/o Asc) served as positive and negative controls, respectively. (*B*) S-nitrosylation of TDP-43 by endogenous NO in HEK-nNOS cells. HEK-nNOS cells were incubated with calcium ionophore A23187 (5 μM) to activate nNOS ($n = 3$). (*C*) S-nitrosylation of TDP-43 by endogenous NO upon NMDA receptor stimulation. Primary rat cortical neurons were exposed to 50 μM NMDA ($n = 4$). Graphs indicate mean + SEM; $^*P = 0.0164$ (*B*), 0.0494 (*C*, control vs. NMDA), and 0.0282 (*C*, NMDA vs. NMDA [w/o Asc]) by two-tailed Student's *t* test.

its accumulation in the insoluble fraction of cell/tissue lysates (3, 39, 40). To determine if S-nitrosylation of TDP-43 contributes to this aggregation, we exposed SH-SY5Y cells to SNOC and fractionated the cell lysate for immunoblot analyses. We used this cell line in order to provide a large number of pure neuronal-like cells. We detected a substantial increase in TDP-43 in the insoluble fraction (Fig. 2*E*). We also exposed the cells to GSNO, another physiological NO donor with greater stability than SNOC, and assessed TDP-43 solubility. Similar to the effect of SNOC, we observed elevated levels of insoluble TDP-43 after exposure to GSNO (*SI Appendix*, Fig. S1*A*). As a control experiment, pretreatment with a soluble guanylyl cyclase (sGC) inhibitor, 1H-[1,2,4]oxadiazolo [4,3,-a] quinoxalin-1-one (ODQ), did not affect the levels of insoluble TDP-43 (*SI Appendix*, Fig. S1*B*). This finding is consistent with the notion that a NO-mediated sGC/cyclic guanosine monophosphate (cGMP) pathway does not play a role in NO-induced TDP-43 aggregation and, instead, protein S-nitrosylation is involved. Additionally, GSNO triggered colocalization of TDP-43 with the cytoplasmic SG marker G3BP (Fig. 2*F*), recapitulating this aspect of TDP-43 proteinopathy.

Next, we exposed rat primary cerebrocortical neurons to SNOC or NMDA and found a significant increase in insoluble TDP-43 compared to control. In contrast, the NO synthase (NOS) inhibitor, L-NAME (L-N^G-nitroarginine methyl ester), abrogated the effect of NMDA (Fig. 2*G*). Collectively, these results are consistent with the notion that activation of the NMDAR-nNOS pathway resulted in generation of endogenous NO and formation of SNO-TDP-43, leading to the appearance of disulfide-mediated HMW/aggregated TDP-43.

S-Nitrosylation at Cys173 or Cys175 Initiates Aggregation of TDP-43 and Compromises RNA Processing. To obtain molecular insight into S-nitrosylation-induced TDP-43 aggregation, we next determined the target cysteine residues of S-nitrosylation. We noted that among the six cysteine residues present in TDP-43, four (Cys173, 175, 198, and 244) resided within partial SNO motifs (32). Accordingly, we generated TDP-43 mutants substituting alanine for each of these cysteines. We then expressed each cysteine mutant or wild-type (WT) TDP-43 in neuronal SH-SY5Y cells. Interestingly, after SNOC exposure the single cysteine mutants exhibited S-nitrosylation levels approximately similar to WT TDP-43. In contrast, among various combination of mutants, TDP-43(C173A/C175A) exhibited a drastic decrease in S-nitrosylation (Fig. 3*A*). Since our mass spectrometry analysis demonstrated that S-nitrosylation occurs at a single site in TDP-43 (Fig. 2*B*), these mutagenesis experiments suggest that either Cys173 or Cys175, but not both, are the predominant target of S-nitrosylation under these conditions.

Next, to determine whether S-nitrosylation of TDP-43 at either Cys173 or Cys175 can mediate NO-induced aggregation, we assessed if TDP-43(C173A/C175A) remains soluble during nitrosative stress. As we had predicted, elimination of these S-nitrosylation sites markedly decreased the amount of TDP-43(C173A/C175A) in the insoluble fraction after exposure to SNOC (Fig. 3*B*). To examine the structural implications of these findings, we considered the recently elucidated structure of TDP-43. TDP-43 consists of an N-terminal domain (NTD), two RNA recognition motifs, RRM1 and RRM2, in addition to a long glycine-rich tail domain, also known as the prion-like or low complexity sequence domain (Fig. 3*C*) (41). The S-nitrosylation sites, Cys173 and Cys175, lie within the RRM1 domain, close to the linker region that connects RRM1 to RRM2 (Fig. 3 *C* and *D*). According to recently solved X-ray crystallographic and NMR spectroscopic structures (31, 42), Cys173 and Cys175 are buried inside and pointing toward the interior of the RRM1 domain (Fig. 3*D*), consistent with the notion that the S-nitrosothiol is contained within the protein structure (43).

Chemically, S-nitrosylation of a single thiol group (but not both thiols) of a vicinal pair of cysteine residues can facilitate disulfide formation (20, 37). Along these lines, Cohen et al. (29) reported evidence for an intramolecular disulfide linkage in TDP-43 between Cys173 and Cys175. We therefore employed molecular dynamics simulations to investigate the potential effects of this disulfide bond on the structure of TDP-43. Our analysis suggests that intramolecular disulfide formation leads to perturbation in the microenvironment near Cys244, residing in the RRM2 domain near the end of the linker region (Fig. 3*D*). This structural change, due to the intramolecular disulfide linkage that occurs after S-nitrosylation of Cys173 or Cys175, appears to increase the probability of surface exposure of Cys244. This conformation would thus favor intermolecular disulfide bond formation between Cys244 on adjacent TDP-43 molecules, consistent with prior reports (30).

Normally, TDP-43 binds to and stabilizes nuclear RNAs, such as HDAC6 mRNA, leading to increased expression of this protein;

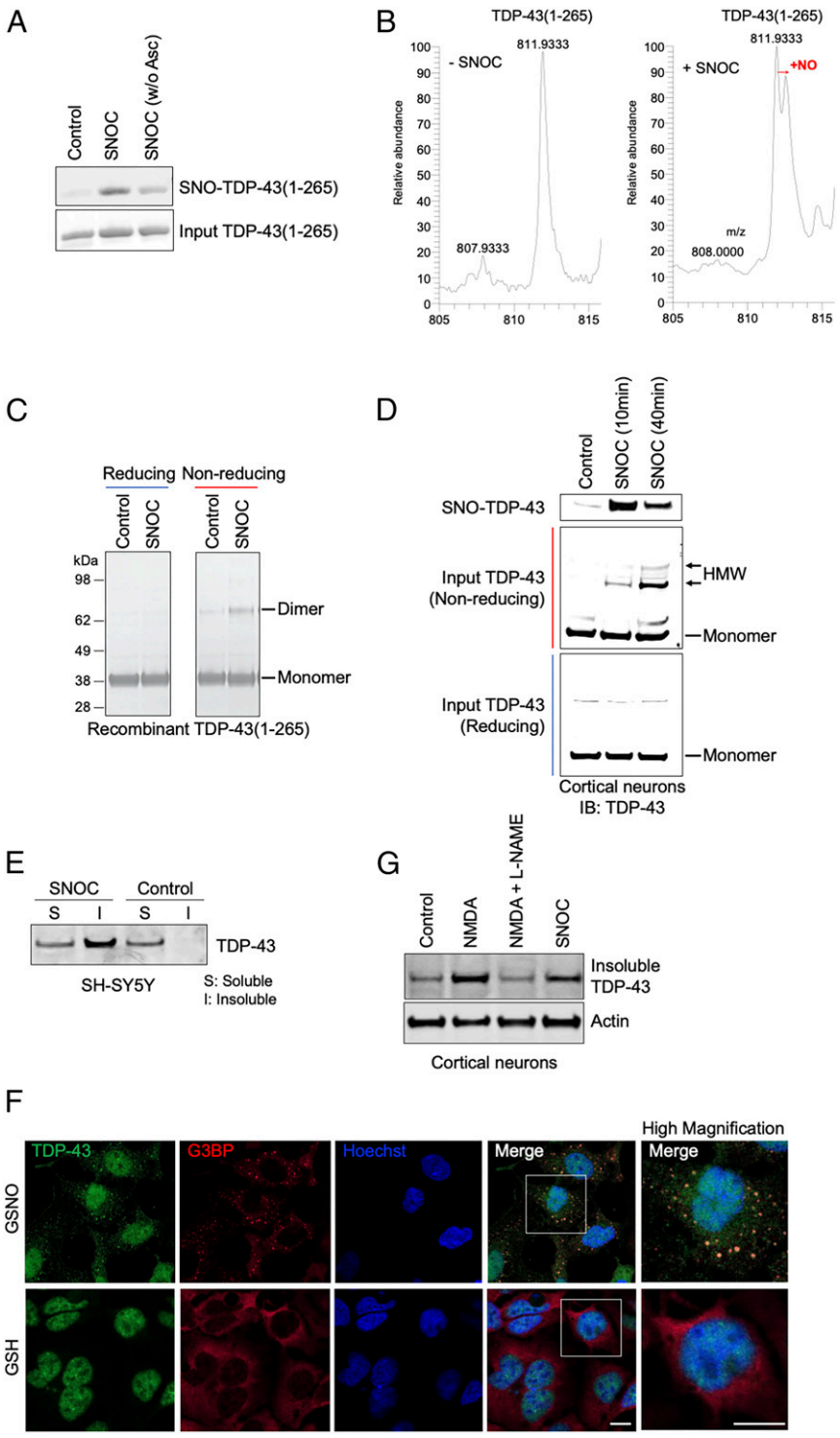

Fig. 2. Nitrosative stress triggers formation of SNO-TDP-43 and HMW TDP-43, stimulating TDP-43 aggregation/insolubility in cell-based assays. (*A* and *B*) S-nitrosylation of recombinant TDP-43 (amino acids 1 to 265, representing the N-terminal fragment of TDP-43). Recombinant TDP-43(1-265) was incubated with or without SNOC (200 μM), subjected to biotin-switch assay (to assess SNO-TDP-43), and analyzed by Coomassie staining for input TDP-43 (*A*). Top-down mass spectrometry analysis identified a single NO modification on TDP-43(1-265). *Left*: Control (without "−SNOC"). *Right*: SNOC exposed (*B*). (*C* and *D*) Exposure to SNOC leads to formation of disulfide-linked, HMW TDP-43. Recombinant TDP-43(1-265) was exposed to SNOC, separated on SDS-PAGE under reducing or nonreducing conditions, and assessed by Coomassie staining. Monomeric (monomer) and dimeric (dimer) species of recombinant TDP-43(aa 1 to 265) are indicated (*C*). Primary rat cortical neurons were exposed to SNOC, and after 10 or 40 min, cell lysates were prepared and subjected to biotin-switch assay for detection of SNO-TDP-43. Total cell lysates were electrophoresed on 4 to 12% gradient SDS-PAGE gels under nonreducing or reducing conditions, and immunoblotted with anti-TDP-43 antibody (*D*). (*E* and *G*) In response to NO exposure, TDP-43 increased in the insoluble fraction of neuroblastoma SH-SY5Y cells (*E*) and primary rat cortical neurons (*G*). SH-SY5Y cells were exposed to SNOC (200 μM), and after 60 min, RIPA soluble (S) and insoluble (I) fractions were prepared. Immunoblots were conducted with anti-TDP-43 antibodies. Primary cultures of rat cortical neurons were exposed to NMDA (50 μM) in the presence or absence of the NOS inhibitor, L-NAME; the insoluble fraction was analyzed by immunoblot. (*F*) Recruitment of TDP-43 into SGs after nitrosative stress. SH-SY5Y cells were exposed to the relatively long-lived NO donor GSNO (200 μM), and after 1 h, immunofluorescence images of G3BP (SG marker, red) and TDP-43 (green) were visualized by confocal microscopy. Boxed area is shown at higher magnification. (Scale bar, 10 μm.)

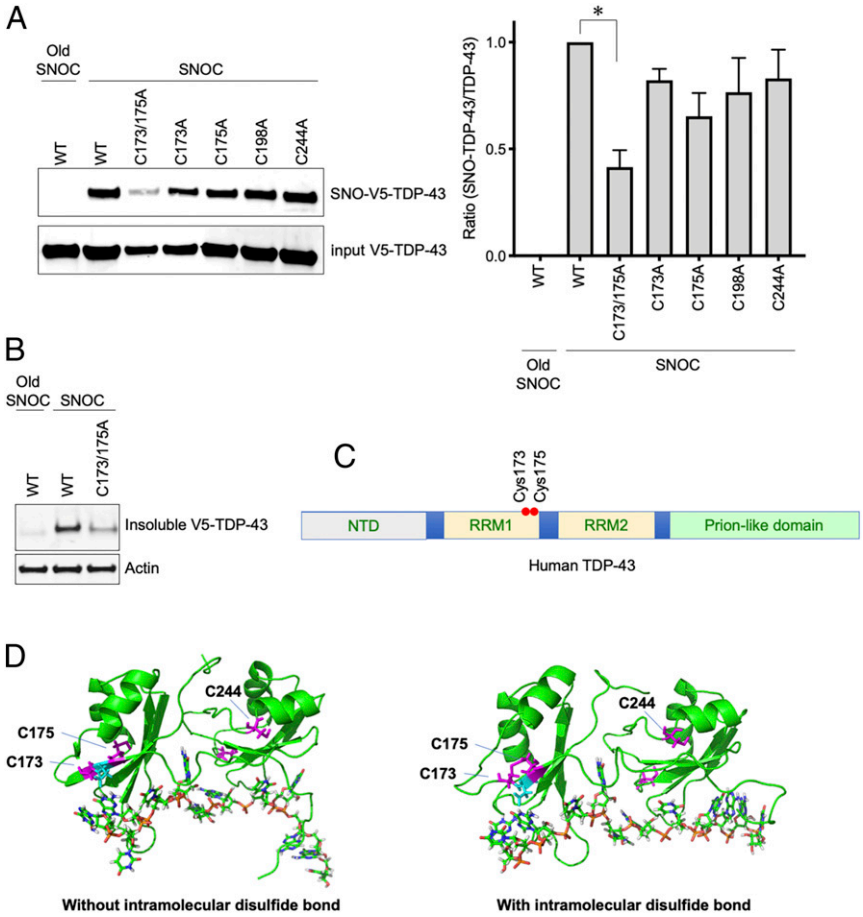

Fig. 3. S-nitrosylation of TDP-43 at Cys173 or Cys175. (*A*) SH-SY5Y cells transfected with V5-tagged WT TDP-43 or Cys to Ala mutants (C173A, C175A, C173A/C175A, C198A, and C244A) were exposed to SNOC. Control cells were exposed to old SNOC, from which NO had been dissipated. After 30 min, SNO-TDP-43 was assessed by biotin-switch assay. *Left*: Immunoblotting with anti-V5 antibody. *Right*: Quantification of SNO-TDP-43 levels ($n = 4$). Graph indicates mean + SEM; $^*P = 0.0066$ by one-way ANOVA, followed by Bonferroni's post hoc test. (*B*) SNOC increases accumulation of insoluble TDP-43 aggregates. SH-SY5Y cells were transfected with V5-tagged WT TDP-43 or TDP-43(C173A/C175A) mutant, and exposed to SNOC (200 μM). RIPA insoluble TDP-43 was detected by immunoblot with anti-V5 antibody. (*C*) Domain structure of human TDP-43. The positions of Cys173 and Cys175 are shown within the RRM1 RNA recognition motif. (*D*) Structure of TDP-43 RRM domains. *Left*: Crystallographic structure of TDP-43 RRM domains (PDB ID: 4BS2) with position of Cys residues 173 and 175 (magenta). *Right*: Snapshot of the TDP-43 RRM structure containing an intramolecular disulfide bond between Cys173 and Cys175 after molecular dynamics simulation.

thus, detection of HDAC6 mRNA levels can serve as another measure to monitor nuclear TDP-43 activity (44, 45). If S-nitrosylated TDP-43 aggregates and becomes mislocalized in cytoplasmic SGs, we would expect a decrease in the normal nuclear activity of TDP-43. Accordingly, we next determined the effects of NO on HDAC6 mRNA expression. Our qRT-PCR analyses revealed that exposure to SNOC led to decreased expression of HDAC6 mRNA in SH-SY5Y cells. In contrast, expression of non-nitrosylatable mutant TDP-43(Cys173A/C175A) prevented the SNOC-induced decrease in HDAC6 mRNA levels (*SI Appendix*, Fig. S2*A*). Additionally, when RNAi was used to decrease the expression of TDP-43, exposure to SNOC did not further decrease HDAC6 mRNA levels (*SI Appendix*, Fig. S2*B*). Taken together, these results are consistent with the notion that S-nitrosylation of TDP-43 inhibits its RNA-stabilizing activity in the nucleus.

Aggregated TDP-43 Spreads from Cell to Cell to Augment Nitrosative Stress, Alter mRNA Expression, and Contribute to Neuronal Injury In Vitro and In Vivo in a NO-Dependent Manner. Importantly, human patient brains with TDP-43 proteinopathy, including FTD and ALS, also manifest increased TDP-43 aggregation in the cytoplasm, thus excluding TDP-43 from the nucleus (46). Mechanism notwithstanding, aggregated, misfolded proteins have previously been shown to trigger the generation of reactive species, including RNS (47, 48), thus contributing to neurotoxicity. To examine if aggregated TDP-43 stimulates production of NO-related species, we overexpressed TDP-43 in SH-SY5Y cells to simulate neurodegenerative conditions (29, 49). We found that enhanced expression of TDP-43 augmented RNS levels, as measured by the Griess reaction. The NOS inhibitor L-NAME significantly blocked this effect, confirming up-regulation of NOS activity as the main cause for the increase in RNS (Fig. 4*A*).

Recent evidence has suggested that oligomeric or aggregated TDP-43 exhibits a prion-like, cell-to-cell spreading phenomenon, acting as a seed to trigger aggregation of TDP-43 in recipient cells (10–12). To investigate if this mechanism could also trigger RNS production, possibly via nNOS, we incubated rat primary cerebrocortical cultures with extracellular recombinant TDP-43(1-265) to simulate aggregation of endogenous TDP-43. Under these conditions, we observed a dramatic increase in neuronal RNS using the fluorescent dye 4-amino-5-methylamino-2',7'-difluorofluorescein diacetate (DAF-FM) to monitor intracellular production of NO-related species (Fig. 4 *B* and *C*). Moreover, we found that exposure to recombinant TDP-43(1-265) triggered cell death in rat primary cerebrocortical neurons, as assayed by terminal deoxynucleotidyl transferase (TdT) dUTP nick-end labeling (TUNEL) assay and

condensed nuclear morphology; importantly, L-NAME reversed this effect (Fig. 4*D*). Taken together, these results are consistent with the notion that spread of aggregated TDP-43 promotes NO production in neighboring neurons, thus constituting a positive feed-forward loop resulting in further enhancement of S-nitrosylation and neurotoxic aggregation of TDP-43.

Next, we investigated whether SNO-TDP-43 could potentially contribute to neuronal cell death. For this experiment, we transfected SH-SY5Y cells with WT or nonnitrosylatable mutant TDP-43, and exposed the cells to a NO donor. By TUNEL assay, we found that exposure to 100 μM SNOC resulted in significantly increased cell death in cells transfected with WT TDP-43, whereas expression of nonnitrosylatable mutant TDP-43 nearly totally protected the cells from the NO-mediated insult (Fig. 4*E*). This finding supports the notion that S-nitrosylation of TDP-43 at Cys173/175 contributes to a signaling pathway leading to neuronal cell death.

Some prior studies have suggested that pathological accumulation of TDP-43 in mitochondria can contribute to TDP-43-associated neurotoxicity (50, 51). Mechanistically, aberrant mitochondrial TDP-43 binds to mRNAs encoding electron transport chain complex I subunits, thereby impairing their translation, and consequently leading to bioenergetic failure and neuronal cell death (50). Others, however, have failed to link mitochondrial TDP-43 to impaired bioenergetics (52). Here, to examine the RNA-binding activity of TDP-43, we determined if S-nitrosylation of TDP-43 affects its interaction with mRNAs encoding mitochondrial complex I subunits. Indeed, we found that exposure of SH-SY5Y cells to SNOC resulted in an increase in TDP-43 immunocomplexed to mRNA encoding mitochondrial complex I subunit ND3 (*SI Appendix*, Fig. S3*A*). In contrast, nonnitrosylatable mutant TDP-43 manifested a decrease in interaction with ND3 mRNA in mitochondria compared to WT TDP-43 (*SI Appendix*, Fig. S3*B*). Next, to simulate the conditions of neurodegenerative disease, we overexpressed WT TDP-43, which also increases NO-related species (Fig. 4*A*), and found that this overexpression of TDP-43 diminished ND3 protein expression via inhibition of translation (*SI Appendix*, Fig. S3 *C* and *D*). In contrast, overexpression of nonnitrosylatable mutant TDP-43 had no effect on ND3 expression (*SI Appendix*, Fig. S3 *C* and *D*), as expected if SNO-TDP-43 were involved in mediation of the effect. In control experiments, we showed that translocation of TDP-43 into mitochondria was not affected by exposure to SNOC or substitution of Cys173/175 to Ala (*SI Appendix*, Fig. S3 *E* and *F*), consistent with the notion that TDP-43 enters mitochondria independently of its S-nitrosylation. Taken together, these findings support the existence of a pathway in which aberrant SNO-TDP-43 (but not nonnitrosylatable mutant TDP-43) affects expression of target mRNAs, including that encoding the ND3 subunit of mitochondrial electron transport chain complex I, an event with potential implications for neuronal vulnerability (50).

Even more critical, however, for the neuropathologic effects of aggregated TDP-43 may be the lack of normal TDP-43 function in the nucleus. For example, emerging evidence suggests that mislocalization and aggregation of TDP-43 in the cytosol in SGs is linked to the aberrant function of this RNA-binding protein by preventing its physiological activity in the nucleus, thus contributing to neurodegeneration (3, 39, 40). Moreover, oxidative modifications of TDP-43 have been reported to drive its sequestration into cytoplasmic SGs (29, 53, 54). Normally, TDP-43 is located in the nucleus where it binds to different classes of RNAs, regulating their processing and stability to help maintain neuronal function (3, 46). Recent studies have demonstrated that nuclear TDP-43 binds to and represses nonconserved cryptic exons; in contrast, abnormal cytoplasmic localization of TDP-43 in FTD/ALS allows pathological expression of cryptic exons, possibly because of decreased availability of TDP-43 in the nucleus (55–58). To examine if S-nitrosylated TDP-43 affects expression of cryptic exons, we used specific primers for a well-characterized cryptic exon in ATG4B precursor RNA. Our qRT-PCR analysis found increased expression of the ATG4B cryptic exon in SH-SY5Y cells after exposure to SNOC under conditions that increase SNO-TDP-43 (*SI Appendix*, Fig. S4*A*). Moreover, similar to this effect, siRNA-mediated knockdown of TDP-43 increased the expression of the ATG4B cryptic exon (*SI Appendix*, Fig. S4 *A* and *B*). These findings are consistent with our hypothesis that S-nitrosylation of TDP-43 leads to its aggregation and sequestration in cytosolic SGs accompanied by its clearance from the nucleus, compromising the ability of TDP-43 activity to repress cryptic exons.

Additional recent studies demonstrated that TDP-43 normally binds to a cryptic exon in human stathmin-2 (STMN2) RNA transcripts, thereby facilitating neuronal expression of STMN2. STMN2 is an important regulator of microtubule dynamics during axonal outgrowth and regeneration and is thus important for neuronal health and survival. Similar to the effects on the ATG4B cryptic exon, lack of nuclear TDP-43 leads to an increase in STMN2 cryptic exon followed by a decrease in normal STMN2 protein expression. Moreover, increased expression of STMN2 cryptic exon was shown to be a primary mediator of TDP-43-associated motor neuron toxicity (57, 58). Along these lines, in the present study we found that extracellular recombinant TDP-43(1-265), which produced neural cell toxicity at least in part via a NO-mediated pathway (Fig. 4), also increased the expression of STMN2 cryptic exon in SH-SY5Y cells, similar to the effects of siRNA-mediated TDP-43 knockdown. Moreover, the TDP-43-mediated increase in STNM2 cryptic exon was totally abrogated by the NOS inhibitor L-NAME (Fig. 5 *A*–*D*).

Next, to examine the effects on neurodegeneration of S-nitrosylation-mediated TDP-43 aggregation in vivo, we employed an animal model of TDP-43 cell-to-cell spread (59). For this purpose, we performed intracerebral injections of recombinant TDP-43(1-265). Four weeks later, we observed evidence for TDP-43 aggregation in the form of phospho-TDP-43-positive cytosolic SGs near the injection site, confirming the apparent seeding activity of the injected recombinant TDP-43(1-265) (Fig. 5*E*). Interestingly, a recent in vitro study suggested that TDP-43-associated neurodegenerative phenotypes are mediated in part via inhibition of the CREB pathway (60). Following up on this finding with in vivo experiments, we observed that intracerebral injection of recombinant TDP-43(1-265) caused a significant decrease in CREB phosphorylation (pCREB), reflecting inhibition of CREB activity in the mouse brains. Critically, this effect was significantly ameliorated by L-NAME (Fig. 5 *F* and *G*). Additionally, L-NAME significantly abrogated the loss of neuron-specific microtubule-associated protein 2 (MAP2) induced by injection of TDP-43(1-265) (Fig. 5 *H* and *I*), consistent with the notion that SNO-TDP-43 contributed to neuronal cell death. This is an in vivo demonstration of a molecular pathway triggered by TDP-43 that engenders a neurodegenerative phenotype, and, in this case, in a NO-dependent fashion. Collectively, these findings are consistent with the notion that NO-related species contribute in vivo not only to pathological aggregation of TDP-43, but also to cell-to-cell propagation, and neurotoxicity.

S-Nitrosylation and Aggregation of TDP-43 in Postmortem Human FTD Brains and hiPSC-Derived Motor Neurons. To confirm that S-nitrosylation and subsequent aggregation of TDP-43 occur in human neurologic disease, we investigated postmortem human brains obtained from FTD patients. By biotin-switch assay, we found statistically increased SNO-TDP-43 levels in human FTD brains but not in control brains (Fig. 6*A* and *SI Appendix*, Fig. S5 *A*–*C*). Critically, this increase was equal to or greater than that encountered in our cell-based models (Fig. 1 *B* and *C*), consistent with the notion that FTD brains contain pathophysiologically relevant amounts of SNO-TDP-43. Additionally, in FTD brains we observed HMW species of TDP-43 that were

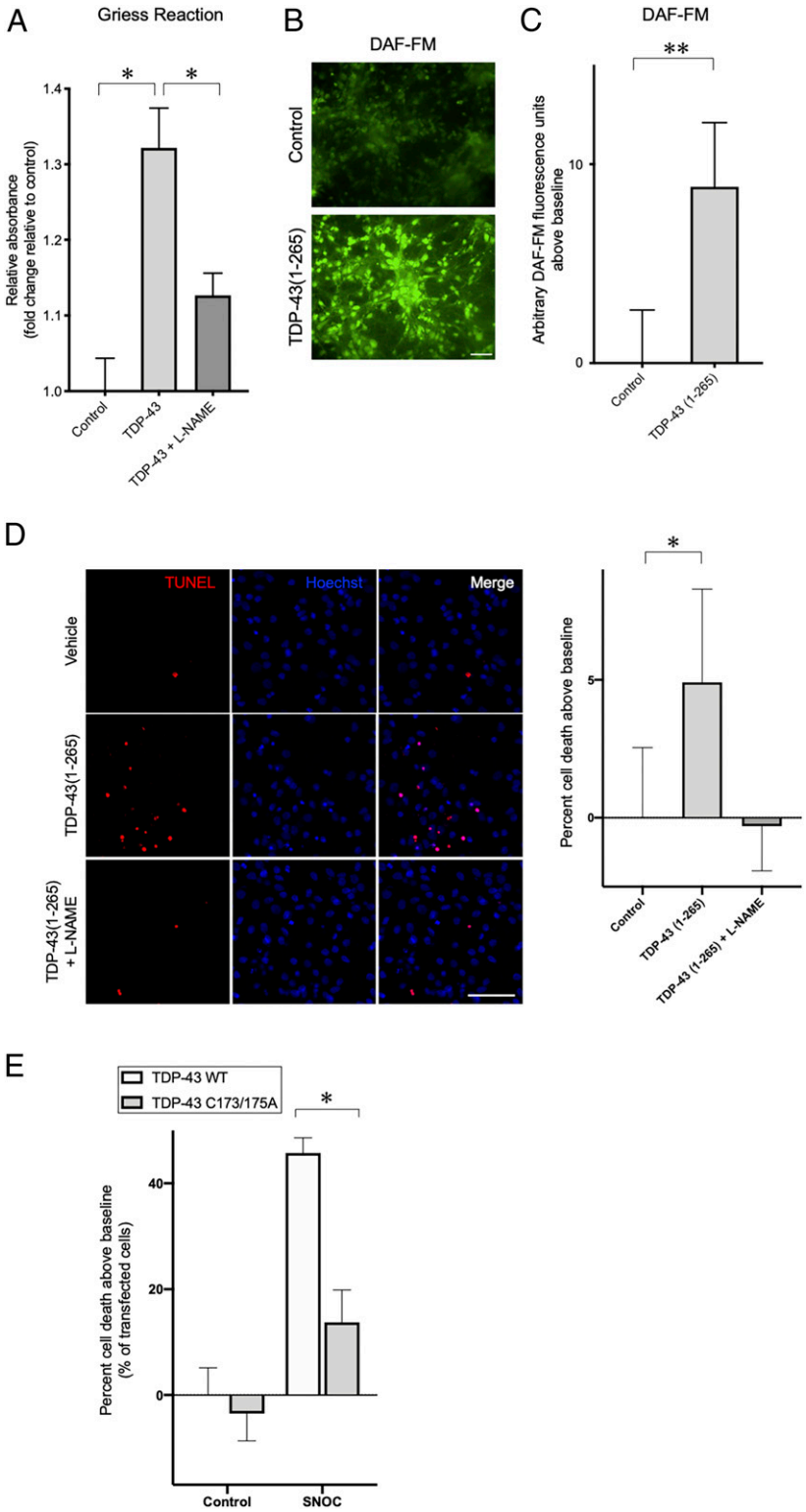

Fig. 4. TDP-43 aggregation induces generation of endogenous NO-related species, and nonnitrosylatable mutant TDP-43 rescues neurotoxicity. (*A*) SH-SY5Y cells were transfected with empty vector (control) or WT TDP-43. To block NOS activity, cells were incubated with L-NAME. Seventy-two hours after transfection, culture medium was collected, and nitrite/nitrate levels were determined using Griess reagent ($n = 4$). (*B* and *C*) Primary rat cortical neurons were exposed to 50 nM recombinant TDP-43(1-265) or control protein (BSA) for 24 h, and the fluorescence response of DAF-FM, an indicator of NO-related species, was measured. Representative images of DAF-FM-labeled cells (*B*). (Scale bar, 50 μm.) Quantification of changes in DAF-FM fluorescence intensity after exposure to recombinant TDP-43(1-265) ($n = 5$) (*C*). (*D*) Primary rat cortical neurons were exposed to 50 nM recombinant TDP-43(1-265) or control protein (BSA) for 72 h, and cell death was measured by TUNEL assay. Representative images of TUNEL-positive cells (*D*, *Left*), and quantification of cell death after exposure to recombinant TDP-43(1-265) ($n = 3$) (*D*, *Right*). (Scale bar, 50 μm.) (*E*) Effects of SNO-TDP-43 on neuronal cell death. SH-SY5Y cells were transfected with WT TDP-43 or TDP-43(C173A/C175A) mutant constructs, exposed to 100 μM SNOC, and analyzed 24 h later for cell death by TUNEL staining ($n = 4$ separate experiments). Graphs indicate mean + SEM; $*P = 0.0033$ (*A*, control vs. TDP-43), 0.0181 (*A*, TDP-43 vs. TDP-43 + L-NAME), 0.0426 (*D*), and 0.0032 (*E*) by two-tailed Student's *t* test. $**P = 0.0336$ (*C*) by one-tailed Student's *t* test.

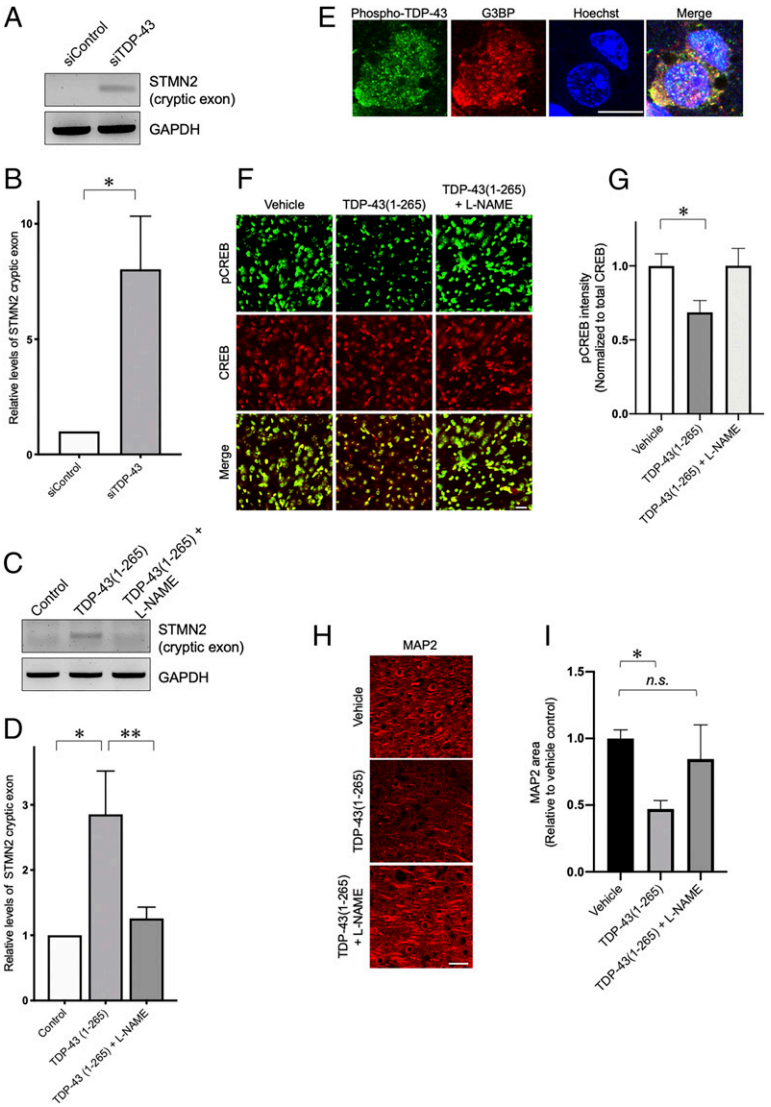

Fig. 5. TDP-43 regulates STMN2 expression and CREB phosphorylation in a NO-dependent manner. (*A* and *B*) Analysis of STMN2 cryptic exon expression in SH-SY5Y cells transfected with TDP-43 siRNA (siTDP-43) ($n = 3$). (*C* and *D*) Exposure of cells to recombinant TDP-43(1-265) increased STMN2 cryptic exon expression; NOS inhibitor L-NAME significantly reversed this effect (*D*, $n = 3$). Expression of STMN2 cryptic exon was monitored by standard RT-PCR (*A* and *C*) and qRT-PCR (*B* and *D*). GAPDH levels were measured by qRT-PCR as an internal standard. (*E*) Intracerebral injection of recombinant TDP-43(1-265) results in appearance of phospho-TDP43-positive cytosolic SGs. Four weeks after injection, confocal immunohistochemical images of phospho-TDP-43 (green) and G3BP (SG marker, red) were obtained in cortical sections adjacent to the injection site. (Scale bar, 10 μm.) (*F* and *G*) Intracerebral injection of recombinant TDP-43(1-265) induced down-regulation of pCREB expression in vivo. Coinjection of L-NAME to block NOS activity abrogated this result. Representative double-labeled immunofluorescence images of pCREB and total CREB (*F*), and quantification of pCREB expression ($n = 27$ brain sections analyzed in nine mice) (*G*). (Scale bar, 20 μm.) (*H* and *I*) Intracerebral injection of recombinant TDP-43(1 to 265) decreases MAP2 expression in vivo. Coinjection of L-NAME abrogated this effect. Representative immunofluorescence images for MAP2-positive neuronal dendrites (*H*), and quantification of MAP2 expression ($n = 27$ brain sections analyzed in nine mice) (*I*). (Scale bar, 40 μm.) Histograms represent mean + SEM; $^*P = 0.0378$ (*B*), $^*P = 0.0222$ (*D*), $^{**}P = 0.0456$ (*D*), $^*P = 0.0258$ (*G*), and $^*P = 0.0042$ (*I*) by Student's *t* test; n.s., not significant.

sensitive to reducing conditions (Fig. 6*B*), suggesting that TDP-43 is aggregated, at least in part, via disulfide linkage in vivo, similar to our in vitro models triggered by the aberrant redox reaction of protein S-nitrosylation of TDP-43.

Prior evidence suggests that both genetic and environmental risk factors, including factors that might possibly increase NO, contribute to the development of ALS/FTD spectrum disorders (61). To test in a human context if genetic variations associated with motor neuron degeneration render neurons more vulnerable to nitrosative stress, we generated hiPSC-derived motor neurons from patient skin biopsies (62). Similar to the other cell-based models described above, exposure to SNOC increased insoluble TDP-43 in WT motor neurons derived from control hiPSCs (Fig. 6*C*). We also generated mutant motor neurons from patient hiPSCs bearing an R155H mutation in the *VCP* gene, which is associated with ALS/FTD and other neurodegenerative diseases (63, 64). *VCP* mutation has been reported to cause a disturbance in autophagic clearance of SGs containing aggregated TDP-43 (65), thus contributing to TDP-43 accumulation in these cells. Remarkably, NO exposure of these mutant hiPSC-derived motor neurons resulted in a dramatic increase in the amount of insoluble TDP-43. The insoluble fraction from the hiPSC-derived neurons included both HMW TDP-43 and cleaved fragments (Fig. 6*C*), similar to that encountered in human postmortem brain tissues (Fig. 6*B*). Additionally, we observed SNO-TDP-43 in these mutant hiPSC-derived motor

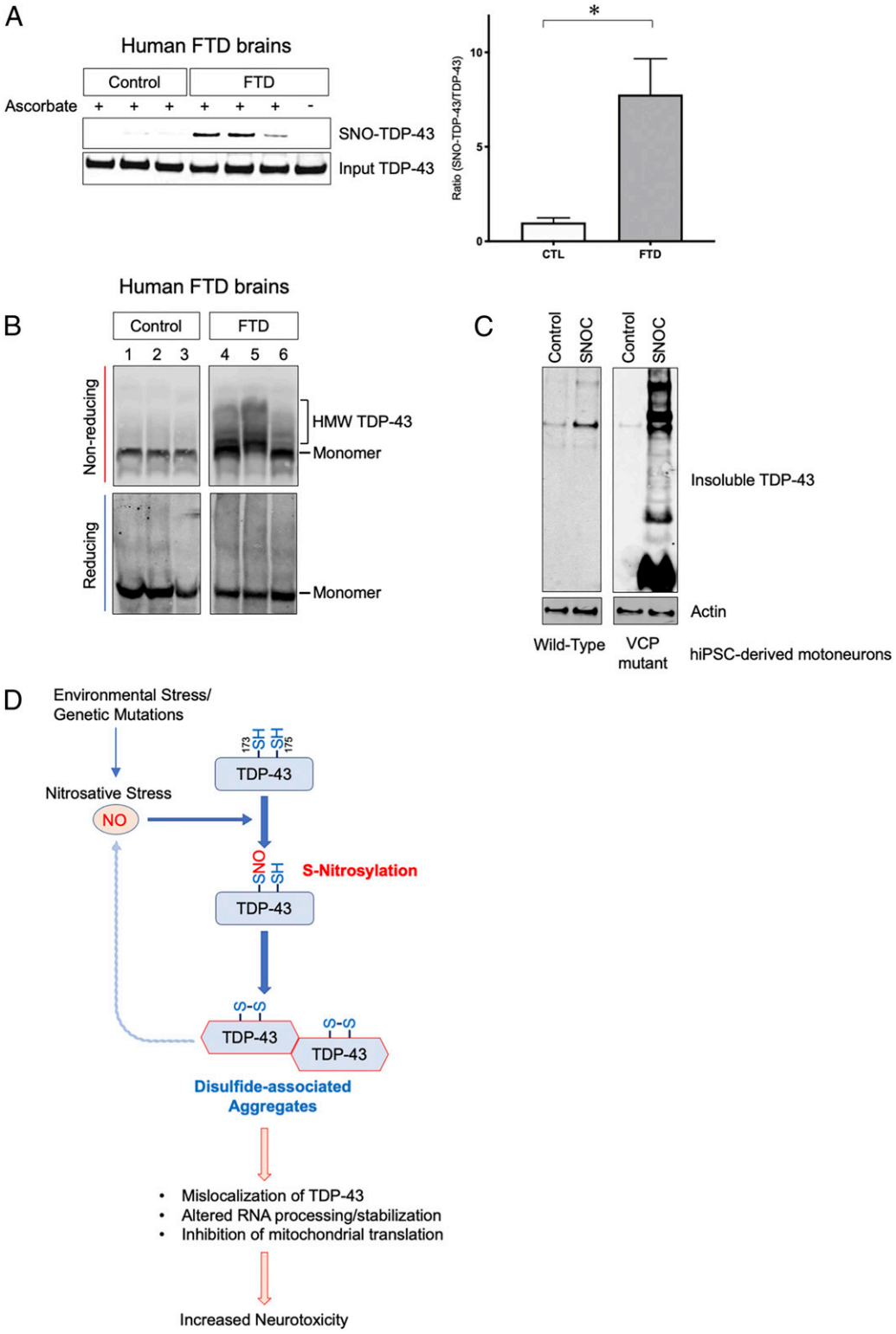

Fig. 6. S-nitrosylation and aggregation of TDP-43 in human FTD brains and hiPSC-derived motoneurons. (*A*) Detection of SNO-TDP-43 by biotin-switch assay in human postmortem brain lysates prepared from control ($n = 9$) and FTD patients ($n = 13$) (*SI Appendix*, Fig. S5 *A–C* and Table S1). Graph indicates mean + SEM; $*P = 0.0080$ by two-tailed Student's t test. (*B*) HMW TDP-43 disulfide species in human FTD brains. Brain lysate was separated by SDS-PAGE under reducing or nonreducing conditions, and immunoblotted with anti-TDP-43 antibody. (*C*) SNOC increases accumulation of insoluble TDP-43 in motor neurons derived from hiPSCs. hiPSCs carrying a mutation in the VCP gene were differentiated into motor neurons and exposed to 100 μM SNOC. Insoluble fractions were analyzed by immunoblot. (*D*) Proposed schema for S-nitrosylation-induced TDP-43 aggregation and neurotoxicity. In neurodegenerative diseases such as ALS/FTD, increased nitrosative stress engenders S-nitrosylation of TDP-43 at Cys173 or Cys175, facilitating intramolecular disulfide bond formation. This reaction contributes to oligomerization/aggregation of TDP-43. Aggregated TDP-43 is cleared from the nucleus and mislocalizes to cytoplasmic SGs and mitochondria. This causes a further increase in NO generation and alterations in RNA processing, stabilization, or translation, contributing to TDP-43 neurotoxicity.

neurons (*SI Appendix*, Fig. S5*D*). These results are consistent with the premise that genetic mutations related to FTD/ALS predispose neurons to SNO-TDP-43 formation and increased aggregation. Overall, our model systems strongly support that NO-mediated aggregation of TDP-43 manifests aberrant activity and contributes to neuronal degeneration.

Discussion

TDP-43 oligomerization, insolubility, and aggregation have been implicated in the pathogenesis of ALS/FTD spectrum diseases. Aggregated TDP-43 becomes sequestered in cytoplasmic SGs, and exclusion of TDP-43 from its normal location in the nucleus leads to aberrant cryptic exon expression for messages such as STMN2 and to decreased CREB activity, with consequent neurotoxic outcome (57, 58, 60). The molecular mechanisms responsible for these cellular events, however, remain only incompletely characterized. Here, we provide evidence that nitrosative stress can be triggered by cell-to-cell spread of TDP-43, and in turn contributes to aggregation and associated neurotoxicity via S-nitrosylation of TDP-43. Importantly, increased nitrosative stress has been shown to occur during normal aging and can be further enhanced by exposure to environmental toxins (47, 66), which may in fact contribute to the pathogenesis of ALS/FTD.

We demonstrate that NO-related species mediating nitrosative stress can S-nitrosylate TDP-43 at Cys173 or Cys175, facilitating disulfide bond-mediated aggregation, thus compromising the normal activity of TDP-43. Additionally, we found a positive feedback mechanism whereby aggregated/misfolded TDP-43 further enhances NO generation to augment this pathogenic cascade. Thus, our findings lead us to propose a pathological model in which aberrant S-nitrosylation of TDP-43 represents a key mediator of TDP-43 aggregation, leading to generation of additional NO-related species and further aggregation, and thus contributing to neurotoxicity in ALS/FTD spectrum disorders (Fig. 6*D*).

Mechanistically, TDP-43 and other heterogeneous nuclear ribonucleoproteins (hnRNPs), including FUS, hnRNPA1, and hnRNPA2, are known to exhibit liquid–liquid phase separation, forming cytosolic SGs via interaction with multiple cellular macromolecules such as protein complexes and RNAs in response to environmental stressors (9, 67). Within these liquid droplet-like/membrane-less organelles, hnRNPs regulate RNA translation, splicing, and decay, as well as dynamic assembly of SG components, thus optimizing expression of stress-responsive mRNAs for neuroprotection (67). Emerging evidence, however, suggests that FTD/ALS-associated mutations in TDP-43 cause aberrant aggregation, leading to less dynamic states of TDP-43 in SGs, thus disturbing normal RNA metabolism and contributing to FTD/ALS pathogenesis (68). Similar to TDP-43 mutation, in the present study we show that increased nitrosative stress triggers S-nitrosylation-dependent aggregation of WT TDP-43, thus altering its RNA-binding activity. Critically, we found high levels of SNO-TDP-43 in human brains of sporadic cases of FTD as well as in our hiPSC models of the disease (Fig. 6 *A* and *C*). Hence, our findings support the premise that SNO-TDP-43 formation in SGs contributes to dysfunction of the membrane-less organelles, thus mimicking the rare genetic mutations that cause the disease.

Chemically, S-nitrosothiols often represent labile modifications of cysteine residues, with the target thiol group frequently undergoing further oxidative reaction, which can include disulfide bond formation with a vicinal cysteine residue (19, 20, 38). Accordingly, following S-nitrosylation of TDP-43, an intramolecular disulfide bond between Cys173 and Cys175 results in a conformational change facilitating aggregation (29, 31). Interestingly, an intermolecular disulfide linkage was recently reported to occur at Cys244 between two TDP-43 protein molecules (30), producing TDP-43 dimers and oligomers (69, 70). In the present study, our molecular dynamics simulations suggested that the intramolecular disulfide bridge that we observed between Cys173 and Cys175 would trigger conformational alterations leading to increased solvent exposure at Cys244, potentially facilitating intermolecular disulfide linkage at that residue. Consistent with this notion, we found empirically that S-nitrosylation of TDP-43 by SNOC or GSNO led to the appearance of reducing-agent-sensitive, HMW TDP-43 species. This experiment represents prima facie evidence for disulfide bond formation between TDP-43 molecules following S-nitrosylation. Critically, we also encountered SNO-TDP-43 and disulfide cross-linked HMW TDP-43 in human FTD brains and patient hiPSC-derived motoneurons, supporting our hypothesis that S-nitrosylation contributes to TDP-43 aggregation under pathophysiologically relevant conditions. Moreover, our findings agree with prior studies showing that TDP-43 forms disulfide-linked aggregates after exposure to cell stress or in the presence of genetic mutations (29, 42, 49, 71).

Additionally, we found in our cell-based models that aggregated TDP-43 resides in the cytoplasm and in mitochondria rather than in its normal, unaggregated nuclear localization. This abnormal localization contributes to aberrant RNA processing/stabilization. Collectively, our findings support the hypothesis that SNO-TDP-43 formation serves as an initial molecular trigger for disulfide-linked aggregation of TDP-43, mislocalization, and functional compromise, contributing to proteinopathy.

Intriguingly, we also present evidence in hiPSC-derived motoneurons that mutation in *VCP*, which has also been linked to ALS/FTD, leads to a dramatic increase in NO-induced TDP-43 aggregation, similar to that observed in postmortem human FTD brains. Moreover, we show that spread of aggregated TDP-43 species between cells increases RNS/NO production in the recipient cells, pointing to a positive feedback loop that enhances SNO-TDP-43-mediated aggregation in a pathological cascade. Taken together, these observations support the notion that aging or environmental risk factors that are known to increase NO-related species, in conjunction with genetic predisposition, may contribute to the pathogenesis of ALS/FTD; importantly, this phenomenon occurs in part via SNO-TDP-43 formation. Hence, both SNO-TDP-43 itself and the signaling cascades associated with SNO-TDP-43 formation may represent potential targets for therapeutic intervention in the ALS/FTD spectrum of disorders.

Materials and Methods

Cell Cultures and Transfections. HEK-293 cells stably expressing nNOS (HEK-nNOS; a gift from David Bredt and Solomon H. Snyder, The Solomon H. Snyder Department of Neuroscience, Johns Hopkins University School of Medicine, Baltimore, MD) and SH-SY5Y cells (ATCC) were grown in Dulbecco's modified Eagle media (DMEM; Life Technologies) supplemented with 10% fetal bovine serum (HyClone), 2 mM L-glutamine (Thermo Fisher Scientific), 50 IU/mL penicillin (Omega Scientific), and 50 μg/mL streptomycin (Omega Scientific) in a humidified atmosphere of 5% CO_2 at 37 °C. For HEK-nNOS cell culture, 100 μg/mL geneticin was added into the culture medium. Transfection of plasmids in HEK-nNOS or SH-SY5Y cell lines was carried out with Lipofectamine 2000 or Lipofectamine LTX with PLUS reagents (Life Technologies), respectively, using protocols recommended by the manufacturer. siRNA transfection was performed with Lipofectamine RNAiMax (Life Technologies) according to the vendor's instructions.

Primary cerebrocortical neurons were harvested from E16 Sprague-Dawley rats and maintained in culture as described previously (35). In brief, dissected cerebrocortices were digested with trypsin, and dissociated cells were plated on poly-L-lysine-coated plates in D10C medium (80% DMEM with high glucose, 10% FBS, 10% F12 [HyClone], 30 mM M Hepes [Omega], 2 mM L-glutamine, and 100 U/mL penicillin, and 100 μg/mL streptomycin). Experiments were performed 14 d after plating (for SNOC) or after 21 d (for NMDA) to ensure development of glutamate receptors on the cell surface. To induce nNOS activation, cerebrocortical cultures were exposed to NMDA (50 μM) plus glycine (5 μM) for 20 min in Earle's balanced salt solution (EBSS). After NMDA exposure, EBSS was replaced with conditioned medium. To inhibit NOS activity, cells were incubated with 1 mM L-NAME. sGC activity was inhibited by ODQ (Sigma, O3636). hiPSC culture and differentiation into human motor neurons were performed as described previously (62).

Human Brain Tissues. Patient brain tissues were obtained postmortem from subjects whose age, postmortem interval, and gender are described in *SI Appendix*, Table S1. Human brain samples were analyzed with institutional permission under the state of California and NIH guidelines. Informed consent was obtained according to procedures approved by the Institutional Review Board at the University of California San Diego School of Medicine. Before analyzing patient-derived data, we used the robust outlier (ROUT) method (72) (Q = 1; GraphPad Prism) to identify outliers; the identified outlier was excluded from the analysis.

Statistical Analyses. Statistical analyses were performed using GraphPad Prism 7 or Microsoft Excel. Statistical comparisons between two groups were performed by unpaired two-tailed Student's *t* test. In some cases where there was prior evidence that an experimental treatment should only act in one direction, a one-tailed test was performed as per statistical guidelines. Differences among multiple groups were assessed by one-way ANOVA, followed by Bonferroni's post hoc test. $P < 0.05$ was considered statistically significant.

Data Availability. All data are available in the text and *SI Appendix*.

ACKNOWLEDGMENTS. We thank Scott R. McKercher (The Scripps Research Institute) for critical reading of the manuscript, Eliezer Masliah (University of California San Diego and National Institute on Aging/NIH) for providing human brain tissue, and Traci Fang-Newmeyer (Sanford Burnham Prebys Medical Discovery Institute) and Weiping Tan (The Scripps Research Institute) for preparing cultures. This work was supported in part by NIH Grants R01 NS086890, DP1 DA041722, R01 DA048882, RF1 AG057409, and R01 AG056259 (to S.A.L.), R01 AG061845 (to T.N.), and P41 GM103533 (to J.R.Y.). Additional funding was provided by a Distinguished Investigator Award from the Brain & Behavior Research Foundation (to S.A.L.) and by the Michael J. Fox Foundation (to S.A.L. and T.N.). G.W.Y. was partially supported by grants from the NIH (NS103172 and HG004659), TargetALS, and the ALS Association.

1. F. B. Gao, S. Almeida, R. Lopez-Gonzalez, Dysregulated molecular pathways in amyotrophic lateral sclerosis-frontotemporal dementia spectrum disorder. *EMBO J.* **36**, 2931–2950 (2017).
2. M. Neumann *et al*., Ubiquitinated TDP-43 in frontotemporal lobar degeneration and amyotrophic lateral sclerosis. *Science* **314**, 130–133 (2006).
3. S. C. Ling, M. Polymenidou, D. W. Cleveland, Converging mechanisms in ALS and FTD: Disrupted RNA and protein homeostasis. *Neuron* **79**, 416–438 (2013).
4. M. J. Winton *et al*., Disturbance of nuclear and cytoplasmic TAR DNA-binding protein (TDP-43) induces disease-like redistribution, sequestration, and aggregate formation. *J. Biol. Chem.* **283**, 13302–13309 (2008).
5. J. Gao, L. Wang, M. L. Huntley, G. Perry, X. Wang, Pathomechanisms of TDP-43 in neurodegeneration. *J. Neurochem.*, 10.1111/jnc.14327 (2018).
6. C. M. Dewey *et al*., TDP-43 aggregation in neurodegeneration: Are stress granules the key? *Brain Res.* **1462**, 16–25 (2012).
7. M. Hasegawa *et al*., Phosphorylated TDP-43 in frontotemporal lobar degeneration and amyotrophic lateral sclerosis. *Ann. Neurol.* **64**, 60–70 (2008).
8. D. Moujalled *et al*., Kinase inhibitor screening identifies cyclin-dependent Kinases and glycogen synthase kinase 3 as potential modulators of TDP-43 cytosolic accumulation during cell stress. *PLoS One* **8**, e67433 (2013).
9. A. Molliex *et al*., Phase separation by low complexity domains promotes stress granule assembly and drives pathological fibrillization. *Cell* **163**, 123–133 (2015).
10. M. S. Feiler *et al*., TDP-43 is intercellularly transmitted across axon terminals. *J. Cell Biol.* **211**, 897–911 (2015).
11. J. Brettschneider, K. Del Tredici, V. M. Lee, J. Q. Trojanowski, Spreading of pathology in neurodegenerative diseases: A focus on human studies. *Nat. Rev. Neurosci.* **16**, 109–120 (2015).
12. T. Nonaka *et al*., Prion-like properties of pathological TDP-43 aggregates from diseased brains. *Cell Rep.* **4**, 124–134 (2013).
13. J. R. Tollervey *et al*., Characterizing the RNA targets and position-dependent splicing regulation by TDP-43. *Nat. Neurosci.* **14**, 452–458 (2011).
14. J. Zhang *et al*., Neurotoxic microglia promote TDP-43 proteinopathy in progranulin deficiency. *Nature* **588**, 459–465 (2020).
15. F. Geser, M. Martinez-Lage, L. K. Kwong, V. M. Lee, J. Q. Trojanowski, Amyotrophic lateral sclerosis, frontotemporal dementia and beyond: The TDP-43 diseases. *J. Neurol.* **256**, 1205–1214 (2009).
16. B. Oskarsson, D. K. Horton, H. Mitsumoto, Potential environmental factors in amyotrophic lateral sclerosis. *Neurol. Clin.* **33**, 877–888 (2015).
17. P. E. A. Ash *et al*., Dioxins and related environmental contaminants increase TDP-43 levels. *Mol. Neurodegener.* **12**, 35 (2017).
18. M. Zufiría *et al*., ALS: A bucket of genes, environment, metabolism and unknown ingredients. *Prog. Neurobiol.* **142**, 104–129 (2016).
19. T. Nakamura *et al*., Aberrant protein S-nitrosylation in neurodegenerative diseases. *Neuron* **78**, 596–614 (2013).
20. D. T. Hess, A. Matsumoto, S. O. Kim, H. E. Marshall, J. S. Stamler, Protein S-nitrosylation: Purview and parameters. *Nat. Rev. Mol. Cell Biol.* **6**, 150–166 (2005).
21. L. J. Ignarro, Biosynthesis and metabolism of endothelium-derived nitric oxide. *Annu. Rev. Pharmacol. Toxicol.* **30**, 535–560 (1990).
22. V. L. Dawson, T. M. Dawson, E. D. London, D. S. Bredt, S. H. Snyder, Nitric oxide mediates glutamate neurotoxicity in primary cortical cultures. *Proc. Natl. Acad. Sci. U.S.A.* **88**, 6368–6371 (1991).
23. J. R. Lancaster, Jr, How are nitrosothiols formed de novo in vivo? *Arch. Biochem. Biophys.* **617**, 137–144 (2017).
24. B. C. Smith, M. A. Marletta, Mechanisms of S-nitrosothiol formation and selectivity in nitric oxide signaling. *Curr. Opin. Chem. Biol.* **16**, 498–506 (2012).
25. T. Nakamura *et al*., Noncanonical transnitrosylation network contributes to synapse loss in Alzheimer's disease. *Science*, 10.1126/science.aaw0843 (2020).
26. W. Group; Writing Group; Edaravone (MCI-186) ALS 19 Study Group, Safety and efficacy of edaravone in well defined patients with amyotrophic lateral sclerosis: A randomised, double-blind, placebo-controlled trial. *Lancet Neurol.* **16**, 505–512 (2017).
27. K. Satoh, Y. Ikeda, S. Shioda, T. Tobe, T. Yoshikawa, Edarabone scavenges nitric oxide. *Redox Rep.* **7**, 219–222 (2002).
28. T. Watanabe, S. Yuki, M. Egawa, H. Nishi, Protective effects of MCI-186 on cerebral ischemia: Possible involvement of free radical scavenging and antioxidant actions. *J. Pharmacol. Exp. Ther.* **268**, 1597–1604 (1994).
29. T. J. Cohen, A. W. Hwang, T. Unger, J. Q. Trojanowski, V. M. Lee, Redox signalling directly regulates TDP-43 via cysteine oxidation and disulphide cross-linking. *EMBO J.* **31**, 1241–1252 (2012).
30. S. O. Rabdano *et al*., Onset of disorder and protein aggregation due to oxidation-induced intermolecular disulfide bonds: Case study of RRM2 domain from TDP-43. *Sci. Rep.* **7**, 11161 (2017).
31. C. K. Chang, M. H. Chiang, E. K. Toh, C. F. Chang, T. H. Huang, Molecular mechanism of oxidation-induced TDP-43 RRM1 aggregation and loss of function. *FEBS Lett.* **587**, 575–582 (2013).
32. J. S. Stamler, E. J. Toone, S. A. Lipton, N. J. Sucher, (S)NO signals: Translocation, regulation, and a consensus motif. *Neuron* **18**, 691–696 (1997).
33. S. R. Jaffrey, H. Erdjument-Bromage, C. D. Ferris, P. Tempst, S. H. Snyder, Protein S-nitrosylation: A physiological signal for neuronal nitric oxide. *Nat. Cell Biol.* **3**, 193–197 (2001).
34. T. Nakamura *et al*., Transnitrosylation of XIAP regulates caspase-dependent neuronal cell death. *Mol. Cell* **39**, 184–195 (2010).
35. T. Uehara *et al*., S-nitrosylated protein-disulphide isomerase links protein misfolding to neurodegeneration. *Nature* **441**, 513–517 (2006).
36. H. Takahashi *et al*., Hypoxia enhances S-nitrosylation-mediated NMDA receptor inhibition via a thiol oxygen sensor motif. *Neuron* **53**, 53–64 (2007).
37. S. Z. Lei *et al*., Effect of nitric oxide production on the redox modulatory site of the NMDA receptor-channel complex. *Neuron* **8**, 1087–1099 (1992).
38. K. Wolhuter *et al*., Evidence against stable protein S-Nitrosylation as a widespread mechanism of post-translational regulation. *Mol. Cell* **69**, 438–450.e5 (2018).
39. Y. Furukawa, K. Kaneko, S. Watanabe, K. Yamanaka, N. Nukina, A seeding reaction recapitulates intracellular formation of Sarkosyl-insoluble transactivation response element (TAR) DNA-binding protein-43 inclusions. *J. Biol. Chem.* **286**, 18664–18672 (2011).
40. L. Liu-Yesucevitz *et al*., Tar DNA binding protein-43 (TDP-43) associates with stress granules: Analysis of cultured cells and pathological brain tissue. *PLoS One* **5**, e13250 (2010).
41. F. Geser *et al*., Clinical and pathological continuum of multisystem TDP-43 proteinopathies. *Arch. Neurol.* **66**, 180–189 (2009).
42. P. J. Lukavsky *et al*., Molecular basis of UG-rich RNA recognition by the human splicing factor TDP-43. *Nat. Struct. Mol. Biol.* **20**, 1443–1449 (2013).
43. P. T. Doulias *et al*., Structural profiling of endogenous S-nitrosocysteine residues reveals unique features that accommodate diverse mechanisms for protein S-nitrosylation. *Proc. Natl. Acad. Sci. U.S.A.* **107**, 16958–16963 (2010).
44. F. C. Fiesel *et al*., Knockdown of transactive response DNA-binding protein (TDP-43) downregulates histone deacetylase 6. *EMBO J.* **29**, 209–221 (2010).
45. S. H. Kim, N. P. Shanware, M. J. Bowler, R. S. Tibbetts, Amyotrophic lateral sclerosis-associated proteins TDP-43 and FUS/TLS function in a common biochemical complex to co-regulate HDAC6 mRNA. *J. Biol. Chem.* **285**, 34097–34105 (2010).
46. T. J. Cohen, V. M. Lee, J. Q. Trojanowski, TDP-43 functions and pathogenic mechanisms implicated in TDP-43 proteinopathies. *Trends Mol. Med.* **17**, 659–667 (2011).
47. S. D. Ryan *et al*., Isogenic human iPSC Parkinson's model shows nitrosative stress-induced dysfunction in MEF2-PGC1α transcription. *Cell* **155**, 1351–1364 (2013).
48. X. T. Du *et al*., Aβ1-16 can aggregate and induce the production of reactive oxygen species, nitric oxide, and inflammatory cytokines. *J. Alzheimers Dis.* **27**, 401–413 (2011).
49. A. Shodai *et al*., Aberrant assembly of RNA recognition motif 1 links to pathogenic conversion of TAR DNA-binding protein of 43 kDa (TDP-43). *J. Biol. Chem.* **288**, 14886–14905 (2013).
50. W. Wang *et al*., The inhibition of TDP-43 mitochondrial localization blocks its neuronal toxicity. *Nat. Med.* **22**, 869–878 (2016).
51. I. Salvatori *et al*., Differential toxicity of TDP-43 isoforms depends on their submitochondrial localization in neuronal cells. *J. Neurochem.*, 10.1111/jnc.14465 (2018).
52. H. Kawamata *et al*., Mutant TDP-43 does not impair mitochondrial bioenergetics in vitro and in vivo. *Mol. Neurodegener.* **12**, 37 (2017).
53. C. Colombrita *et al*., TDP-43 is recruited to stress granules in conditions of oxidative insult. *J. Neurochem.* **111**, 1051–1061 (2009).

54. J. Meyerowitz *et al*., C-Jun N-terminal kinase controls TDP-43 accumulation in stress granules induced by oxidative stress. *Mol. Neurodegener.* **6**, 57 (2011).
55. J. P. Ling, O. Pletnikova, J. C. Troncoso, P. C. Wong, TDP-43 repression of non-conserved cryptic exons is compromised in ALS-FTD. *Science* **349**, 650–655 (2015).
56. M. Sun *et al*., Cryptic exon incorporation occurs in Alzheimer's brain lacking TDP-43 inclusion but exhibiting nuclear clearance of TDP-43. *Acta Neuropathol.* **133**, 923–931 (2017).
57. Z. Melamed *et al*., Premature polyadenylation-mediated loss of stathmin-2 is a hallmark of TDP-43-dependent neurodegeneration. *Nat. Neurosci.* **22**, 180–190 (2019).
58. J. R. Klim *et al*., ALS-implicated protein TDP-43 sustains levels of STMN2, a mediator of motor neuron growth and repair. *Nat. Neurosci.* **22**, 167–179 (2019).
59. S. Porta *et al*., Patient-derived frontotemporal lobar degeneration brain extracts induce formation and spreading of TDP-43 pathology in vivo. *Nat. Commun.* **9**, 4220 (2018).
60. J. J. Herzog *et al*., TDP-43 dysfunction restricts dendritic complexity by inhibiting CREB activation and altering gene expression. *Proc. Natl. Acad. Sci. U.S.A.* **117**, 11760–11769 (2020).
61. A. Al-Chalabi, Perspective: Don't keep it in the family. *Nature* **550**, S112 (2017).
62. F. J. Martinez *et al*., Protein-RNA networks regulated by normal and ALS-associated mutant HNRNPA2B1 in the nervous system. *Neuron* **92**, 780–795 (2016).
63. J. O. Johnson *et al*.; ITALSGEN Consortium, Exome sequencing reveals VCP mutations as a cause of familial ALS. *Neuron* **68**, 857–864 (2010).
64. G. D. Watts *et al*., Inclusion body myopathy associated with Paget disease of bone and frontotemporal dementia is caused by mutant valosin-containing protein. *Nat. Genet.* **36**, 377–381 (2004).
65. J. R. Buchan, R. M. Kolaitis, J. P. Taylor, R. Parker, Eukaryotic stress granules are cleared by autophagy and Cdc48/VCP function. *Cell* **153**, 1461–1474 (2013).
66. S. Rizza *et al*., *S*-nitrosylation drives cell senescence and aging in mammals by controlling mitochondrial dynamics and mitophagy. *Proc. Natl. Acad. Sci. U.S.A.* **115**, E3388–E3397 (2018).
67. M. D. Purice, J. P. Taylor, Linking hnRNP function to ALS and FTD pathology. *Front. Neurosci.* **12**, 326 (2018).
68. J. P. Taylor, R. H. Brown Jr, D. W. Cleveland, A. L. S. Decoding, Decoding ALS: From genes to mechanism. *Nature* **539**, 197–206 (2016).
69. M. Vivoli-Vega, P. Guri, F. Chiti, F. Bemporad, Insight into the folding and dimerization mechanisms of the N-terminal domain from human TDP-43. *Int. J. Mol. Sci.* **21**, (2020).
70. Y. Shiina, K. Arima, H. Tabunoki, J. Satoh, TDP-43 dimerizes in human cells in culture. *Cell. Mol. Neurobiol.* **30**, 641–652 (2010).
71. L. Bargsted *et al*., Disulfide cross-linked multimers of TDP-43 and spinal motoneuron loss in a TDP-43^{A315T} ALS/FTD mouse model. *Sci. Rep.* **7**, 14266 (2017).
72. H. J. Motulsky, R. E. Brown, Detecting outliers when fitting data with nonlinear regression - a new method based on robust nonlinear regression and the false discovery rate. *BMC Bioinformatics* **7**, 123 (2006).